Nanoscale

Accepted Manuscript

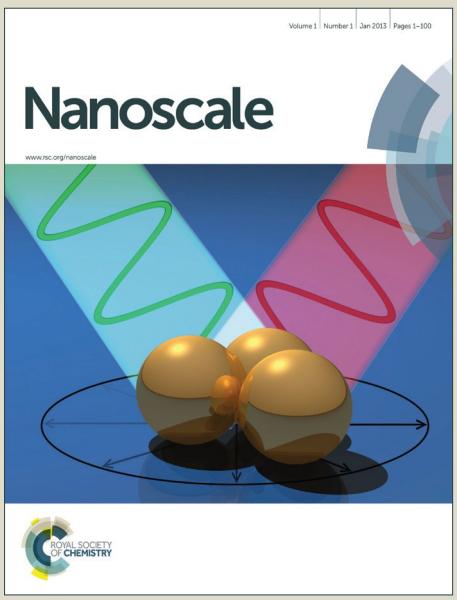

ROYAL SOCIETY OF CHEMISTRY

www.rsc.org/nanoscale

Nanoscale

ARTICLE

Progesterone Binding Nano-Carriers Based on Hydrophobically Modified Hyperbranched Polyglycerols

Received 00th January 20xx,
Accepted 00th January 20xx

DOI: 10.1039/x0xx00000x

www.rsc.org/

M. Alizadeh Noghani [a] and D. E. Brooks [a, b,*]

Progesterone (Pro) is a potent neurosteroid and promotes recovery from moderate Traumatic Brain Injury but its clinical application is severely impeded by its poor water solubility. Here we demonstrate that reversibly binding Pro within hydrophobically modified hyperbranched polyglycerol (HPG-C_n-MPEG) enhances its solubility, stability and bioavailability. Synthesis, characterization and Pro loading into HPG-C_n-MPEG is described. The release kinetics are correlated with structural properties and the results of Differential Scanning Calorimetry studies of a family of HPG-C_n-MPEGs of varying molecular weight and alkylation. While the maximum amount of Pro bound correlates well with the amount of alkyl carbon per molecule contributing to its hydrophobicity, the dominant first order rate constant for Pro release correlates strongly with the amount of structured or bound water in the dendritic domain of the polymer. The results provide evidence to justify more detailed studies of interactions with biological systems, both single cells and in animal models.

Introduction

Traumatic Brain Injury (TBI) is a significant public health problem and an important cause of death and disability in North American adults under the age of 40.[1] TBI has been established as a risk factor for Alzheimer's disease (AD) through linkage with pathologically confirmed AD in several individual case reports.[2,3] Therefore, TBI presents significant short and long-term challenges to worldwide health. The brain injury cascade initiates rapidly as a result of forces that produce tissue distortion at the moment of injury, which can cause long-lasting physical and psychological dysfunction in both mild and severe cases.[4,5] These deformations lead to a primary injury that directly affects blood vessels, axons, neurons and glia. Followed by that, secondary processes cause complex inflammatory, cellular, neurochemical and metabolic modifications.[6,7]

There is no established pharmaceutical agent that enhances functional outcomes following TBI. However, progesterone (Pro) has been reported[8] as the first agent to exhibit strong clinical efficacy as a treatment to promote recovery from moderate TBI and seems to play a beneficial role in the injured brain. Preclinical and clinical research has shown that mortality of brain-injured patients treated with continuous intravenous injection of Pro can be reduced by over 60%, compared to the placebo controls. The major challenge to widespread use of Pro for TBI is its insolubility in aqueous-based formulation due to its hydrophobicity. This contributes to the inability to acutely administer Pro after injury or to store and transport stable formulations of the hormone.[8,9]

Nanoparticles can serve as drug delivery vehicles, offering several advantages over conventional delivery modes by maintaining the optimum therapeutic concentration of drug in the blood or cells which increases patient satisfaction as a result of reduction in frequency of dosing.[10,11] As previously reviewed, polymer micelles ranging from 20 to 100 nm in diameter comprising a hydrophobic core and hydrophilic shell can encapsulate hydrophobic molecules, such as drugs and hormones in the core through hydrophobic interactions, whereas the hydrophilic shell keeps the system soluble in water. The surface of the carriers can be designed to avoid recognition by host defence systems and this leads to longer circulation half-lives.[12-15] However, their structural properties are due to non-covalent interactions among the individual amphiphilic molecular components so their stability is limited to concentrations above a Critical Micelle Concentration which is often not maintained as they are diluted in the blood

[a] *Centre for Blood Research and Departments of Chemistry, University of British Columbia, Vancouver, BC, Canada V6T 1Z3*
[b] *Centre for Blood Research and Departments of Chemistry and of Pathology and Laboratory Medicine, University of British Columbia, Vancouver, BC, Canada V6T 1Z3*
[c] **(D.E.B) phone: 604-822-7081; Email: don.brooks@ubc.ca*

Electronic Supplementary Information (ESI) available: [Figure S-1: Chemical structure of Progesterone (Pro). Figure S-2: ^{1}H NMR spectrum of HPG-C_8-MPEG. Figure S-3: GPC chromatogram of HPG-C_8-MPEG. Figure S-4: ^{1}H NMR spectrum of HPG-C_{12}-MPEG. Figure S-5: GPC chromatogram of HPG-C_8-MPEG. Figure S-6: FTIR spectrum of HPG-C_8-MPEG. Figure S-7: Inverse-gated ^{13}C NMR spectrum of HPG-C_8-MPEG in methanol-d_4. Figure S-8: Semi-log plot to determine initial rapid release kinetics for HPG-C_8-MPEG/Pro in PBS. Figure S-9: Semi-log plot to determine secondary slow release kinetics for HPG-C_8-MPEG/Pro in PBS. Figure S-10: Semi-log plot illustrating the kinetics of Pro release from HPG-C_8-MPEG/Pro in plasma. Figure S-11: Dependence of k_1 and V_p-V_a. Figure S-12: Correlation between the maximum binding capacity of HPG-Cn-MPEG polymeric systems for binding Pro and their total mass of alkyl carbon external to the oxygen (R2 = 0.77 and $p < 0.025$) Table S-1: Effect of loaded Pro on HPG-C_n-MPEG size. Figure S-13. DLS size determination of HPG-C_{10}-MPEG at 2 mg/ml (on the left) and HPG-C_{10}-MPEG/Pro at 2 mg/ml of polymer and 25 µg/ml of Pro (on the right). The minor population of larger particles was reduced in diameter by Pro binding, illustrated above, consistent with an earlier report[11].] See DOI: 10.1039/x0xx00000x

stream. We therefore have focused on hyperbranched (dendritic) hydrophilic polymers derivatized with hydrophobic carbon chains that have been developed to overcome the instability of conventional polymer micelles in the blood stream and therefore have been designated by some as "unimolecular micelles".[16] Their natural stability to environmental effects such as dilution, shear force, and pH, combined with their binding capacity, makes these formulations excellent drug delivery candidates. Moreover, these systems are smaller, with hydrodynamic radii less than 10 nm and have correspondingly low intrinsic viscosities; they are denser and diffuse faster than conventional polymer micelles. Like other carriers the shell of these molecules can be derivatized with suitable functionalities for enhanced drug delivery.[17-22]

This work uses well defined high molecular weight hyperbranched polyglycerols (HPGs) as drug delivery vehicles as they are known to be hydrophilic, blood compatible, non-immunogenic and non-toxic with no evident animal toxicity.[23-34] Unlike many other polymers and carriers used in nanomedicine, HPGs have shown very limited organ accumulation after intravenous injection,[26,29] and are inexpensive and easy to synthesize with good polymerization control. Hydrophobically derivatized HPGs (HPG-C_n-MPEG) have been shown to be efficient drug delivery systems for paclitaxel as well as effectively binding other hydrophobic molecules, such as fatty acids and pyrene.[10] We have synthesized HPG with a hydrophobic character by including some branches terminated with alkyl groups, the polymer as a whole protected by methoxy polyethylene glycol (MPEG) to enable drug binding while enhancing the solubility of the drug and stability of the formulation (HPG-C_n-MPEG); none of the alkylated HPGs are water soluble without significant MPEG derivatization. It has been demonstrated that the binding ability for palmitic acid, paclitaxel and other hydrophobic molecules depends on the alkyl content, thought to associate into a hydrophobic pocket in the polymers, which can be easily manipulated by adjusting the polymer composition during synthesis.[10,11,34]

Pro, being strongly hydrophobic, is a good candidate molecule for formulation into a drug-delivery system based on HPG-C_n-MPEGs. Synthesis and characterization of these polymers, their binding equilibria and release kinetics for Pro are described. The effects of performing the measurements in the biological medium of human plasma, which contains a complex mixture of proteins and other biomolecules, are also investigated. A detailed study of the release kinetics of Pro from a family of HPG-C_n-MPEGs of various molecular weights and alkyl chain size and content provides insights into the structural determinants of the first order rate constants for release. The dominant rate constant correlates very strongly with the amount of structured or bound water within the dendritic domain.

Materials and Methods

Materials and Analytical Methods

1,2-epoxydecane was purchased from TCI America Ltd. (Portland, OR, USA), while all other chemicals were purchased from Sigma-Aldrich Canada Ltd. (Oakville, ON) and used without further purification unless noted. Glycidol (96%) was purified using vacuum distillation and stored over molecular sieves at 4 ^{o}C. 1,2-epoxyoctadecane was synthesized through the peroxidation of octadecane with m-chloroperbenzoic acid. Methoxy polyethylene glycol 350 (MPEG-epoxide) was synthesized from a reaction of MPEG 350, sodium hydroxide and epichlorohydrin, followed by filtration of sodium sulfate and evaporation of excess epichlorohydrin and the solvent as described previously. [10] Proton and carbon NMR spectra were recorded on a Bruker Avance 300 and 400 MHz NMR spectrometer, respectively, using deuterated solvents ($CDCl_3$ and MeOD), with the solvent peak as a reference. Molecular weights and polydispersities of the polymers were measured by gel permeation chromatography (GPC) and a DAWN-EOS multiangle laser light scattering (MALLS) detector; details have been reported elsewhere.[25] Dialysis cassettes were purchased from Thermo Scientific (Rockford, IL). Progesterone powder was obtained from Steraloids Inc. (Newport, RI, USA). A reverse-phase Ultra Pressure Liquid Chromatography system (UPLC) with a symmetric C_{18} column (Acquity BEH C_{18}, Waters) was used for measuring the concentration of Pro bound into and released from HPGs using a gradient mobile phase of water and acetonitrile (ACN) with 0.1% formic acid.

Synthesis of hydrophobically derivatized hyperbrached polyglycerol

The synthetic method has been reported previously.[10] Briefly, polymerization was carried out in a three neck round bottom flask, equipped with a mechanical stirrer and under argon atmosphere, through a simple single-pot synthetic procedure based on ring opening polymerization of epoxide. Initially, 120 mg of the initiator, 1,1,1-Tris(hydroxylmethyl)propane was added to the flask, followed by addition of 0.1 ml potassium methylate solution in methanol (25%w/v). The mixture was stirred at 60 ^{o}C using a magnetic stir bar for 30 minutes then the excess methanol was removed under vacuum. The flask was subsequently kept in the oil bath at 95-100 ^{o}C. Eight millilitres of glycidol and 5 ml of 1,2-epoxyalkane (C_n, n = 6, 8, 10, 12, 14) mixture were added drop-wise over a period of 12 hrs, using a syringe pump under argon. In this step, some of the numerous hydroxyl end groups (given approximately by the degree of polymerization plus the number of OH groups in the initiator) were derivatized with C_n alkyl chains. After completion of monomer addition, the mixture was stirred for an additional 5 hrs. (In the case of solid 1,2-epoxyoctadecane, the monomer was added to the system after the complete addition of glycidol, and the mixture was stirred for 24 hrs under argon). To this mixture, about 20 ml of MPEG-epoxide 350 was added drop-wise and the mixture stirred at 95-100 °C for another 24 hrs under argon.

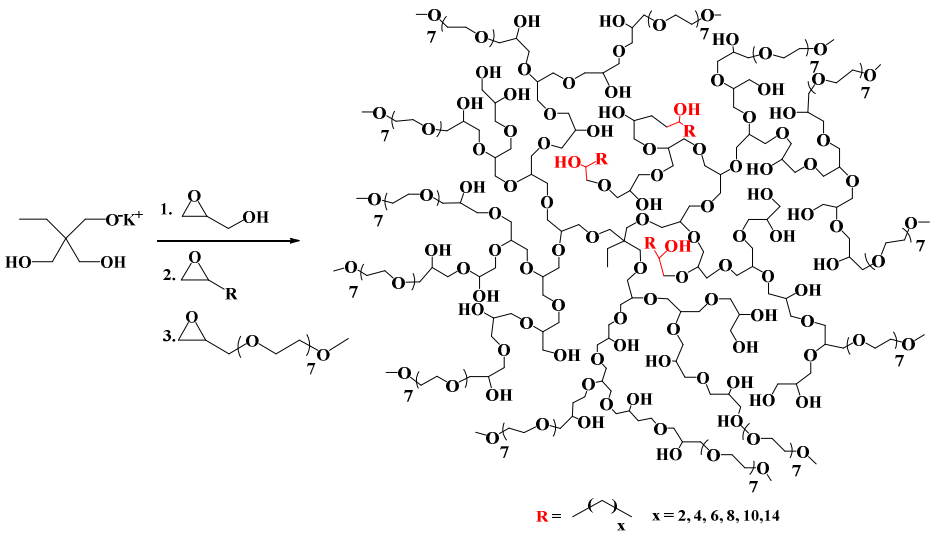

Figure 1. Synthesis scheme of HPG-C_n-MPEG (n = 6, 8, 10, 12, 14, 18); R refers to the hydrophobic chain of the alkyl monomer and x refers to the CH_2 repeating units of the R chain

Polymer was dissolved in methanol and neutralized by passing three times through a cation exchange column (Figure 1). Unreacted alkyl epoxide was removed by extracting with hexane. Methanol was then removed and polymer was dialyzed for 2 days against water. The dry polymer was finally obtained by freeze drying.[10] The mole fractions of glycidol, MPEG and alkyl monomers per polymer were calculated from the ^{1}H NMR spectra; the number of OH groups per molecule can be estimated assuming on average ~one OH group per glycidol monomer from published ^{13}C NMR data.[25] The number of alkyl chains and OH/glycidol groups per molecule were calculated using:

$$n_i = \frac{M_n f_i}{\sum f_i M_i} \quad [1]$$

where:

n_i = number of moles of monomer i in polymer molecule; i refers to glycidol, alkyl or MPEG

f_i = mole fraction of monomer i in polymer molecule

M_i = molecular weight of monomer i incorporated in polymer molecule

M_n = number average molecular weight of polymer

The sum is taken over all monomer species in the molecule. Note that the total content of monomer groups per polymer molecule, n_T, is given by:

$$n_T = \frac{M_n}{\sum f_i M_i} \quad [2]$$

Total mass of alkyl carbon in each system was calculated by multiplying the number of alkyl chains with the number of carbons in the alkyl epoxide monomer, n. In order to correlate the effects of hydrophobic modification on polymer behaviour, the number of purely hydrophobic carbons per chain (R) was used for calculations which is (n-2) carbons, without considering the two carbons originating from the epoxide ring of the epoxyalkane monomer separated by the epoxide oxygen from the linear hydrophobic chain. Molecular weights, polydispersities and hydrodynamic radii of the polymers were measured by GPC. A fractionation method was applied using diethyl ether as the precipitant. Increasing ratios of diethyl ether were added to the remaining polymer solutions in methanol to provide more uniform molecular weight distributions and narrower polydispersities as described previously.[35] Chemical characteristics of HPG-C_n-MPEGs polymeric systems are summarized in Table 1.

Hydration of HPG-C_n-MPEG

Since hydration of HPG-C_n-MPEGs could influence their drug binding and release, the amount of non-freezing water bound to, or structurally altered by, the polymers was measured using Q2100 differential scanning calorimetry (DSC) (TA instruments, New Castle, DE, USA). The method has been described previously [36,37] and as the temperature is ramped up from -20 °C assesses the reduction in heat absorbed around 0 °C when water melts in the presence of polymer. Briefly, about 20 µl of 5% or 10% w/w (polymer-water) solution were cooled down to -20 °C, followed by heating up to -5 °C at the rate of 2 °C /min. The sample heating was continued from -5 °C to +5 °C at the rate of 0.2 °C/min and at 2 °C/min to +20 °C thereafter. The heat flow (J/g) was recorded as a function of temperature and the enthalpy of fusion of water was calculated from the integration of the area under the peak and compared to the pure water as a control. The moles of water bound or altered per mole of HPG-C_n-MPEG, N, was then calculated from the following equation:

$$N = \frac{\left((\Delta H_0(1-C_p)-\Delta H_p)M_n\right)}{\left(\Delta H_0 18.02 C_p\right)} \quad [3]$$

Where, ΔH_0 is the fusion enthalpy of pure water, ΔH_p is the fusion enthalpy of free water in the polymer solution, M_n is the

Table 1. Characteristics of HPG-C_n-MPEG

HPG-C_n-MPEG	C_n mol%[a]	MPEG mol%[a]	M_n (10^3g/mol)	M_w / M_n	No. of alkyl chains/ polymer molecule	No. of hydrophobic carbons (R)/ polymer molecule	$R_{h\ avg}$[b] (nm)	Yield%
HPG-C_6-MPEG	30	29	68	1.98	115	460	6.8 (± 0.24%)	61
HPG-C_8-MPEG	28	36	99	1.26	137	822	4.4 (± 0.41%)	74
HPG-C_{10}-MPEG	15	31	110	1.74	89	712	5.5 (± 0.27%)	68
HPG-C_{12}-MPEG	12	30	168	1.82	111	1110	7.8 (± 0.03%)	76
HPG-C_{14}-MPEG	9	34	125	1.92	60	720	6.7 (± 0.24%)	71
HPG-C_{18}-MPEG	3	30	113	1.47	17	272	7.5 (± 0.24%)	69

[a]: Mole fractions of alkyl and MPEG monomers are calculated from proton NMR; Number of hydrophobic carbons in R chain = (n-2) per polymer molecule is calculated from multiplying the number of alkyl chains per polymer molecule by the number of carbons in R chain (n-2). [b]: Hydrodynamic radii are calculated from dynamic light scattering (QUELS), GPC

molecular weight of the polymer, and C_p is the mass fraction of HPG-C_n-MPEG in the solution. Controls were run with HPG-MPEG (M_n = 93,000; PDI = 1.56; MPEG content 27%).

Incorporation of Pro into HPG-C_n-MPEGs

For each HPG-C_n-MPEG preparation, the binding capacity for Pro and the stability (half-life) of the binding in buffer or plasma were studied. Different concentrations of Pro (Figure S-1) and a constant concentration of HPG-C_n-MPEGs were dissolved in ACN, dried in an oven at 60 °C for 60 minutes and flashed with a nitrogen stream for a few minutes to eliminate traces of the organic solvent. The resulting HPG-C_n-MPEG/Pro mixture was hydrated with 10 mM phosphate buffered saline (PBS - 137 mM NaCl, 2.7 mM KCl, 10 mM Na_2HPO_4 and 1.8 mM KH_2PO_4) at pH 7.4 and vortexed for few minutes. The loaded carriers were purified by double filtration with a 0.2 µm syringe filter to remove precipitated Pro. All HPG-C_n-MPEG/Pro solutions were used on the same day as they were prepared. The concentration of Pro was varied from 50 to 375 µg/ml, while the concentration of HPG-C_n-MPEG was held constant at 20 mg/ml. The maximum loading capacity and stability of Pro loaded in HPG-C_n-MPEGs were determined by gradient reverse-phase UPLC. Similarly, the stability of Pro loaded into HPG-C_n-MPEG was evaluated within 24 hrs.

Drug quantification study

The amount of Pro incorporated into HPG-C_n-MPEG was determined by gradient reverse-phase UPLC, as established previously for similar hydrophobic drugs such as paclitaxel and docetaxel.[34, 38-39] Drug content analysis was performed using a symmetric C_{18} column (1.7 µm, 2.1×50 mm) with two mobile phases containing 0.1% formic acid in water (mobile phase A) and 0.1% formic acid in ACN (mobile phase B) at a flow rate of 0.3 ml/min. Composition of mobile phases was set from the initial to 1.50 min at 70% A and 30% B, followed by changing from 1.50 - 2.10 min at 5% A and 95% B, and back to 70% A and 30% B from 2.10 min towards the end. Sample injection volumes were 20 µl and Pro detection was performed using ultraviolet detection at a wavelength of 240 nm. The total run time was set to 4.5 minutes and the Pro retention time was 1.9 minutes. Regarding the precision and linearity, this UPLC method was validated by standard protocols and all samples were diluted to concentrations within the linear range of calibration. The limit of quantification for Pro was 1 µg/ml with a linear dynamic range of 1-100 µg/ml.

Does Pro cause HPG to aggregate?

In an earlier publication from our group[10] we showed that this class of HPG-C_{18}-MPEG molecules did not form micelles in either the presence or absence of a hydrophobic guest molecule, pyrene, over a huge polymer concentration range (0-150 mg/ml). Other systems of amphoteric dendritic molecules have been shown to aggregate above a critical concentration with an attendant large increase in hydrophobic binding into the micellar form, however, at concentrations in the 10^{-1}-10^{-2} mg/ml range [40,41] In the present case, in order to investigate whether the loaded hydrophobic drug causes any aggregation of the polymeric system, we measured the size (R_h value) for the polymer, before and after loading drug at different concentrations typical of critical aggregation values in other dendritic systems. Samples were prepared in 0.1 M $NaNO_3$ and directly injected into the flow cell in a light scattering batch experiment using the MALLS detector. To make the stock solution, 250 µg/ml Pro was loaded on 20 mg/ml HPG-C_{10}-MPEG in ACN, followed by evaporation of solvent and hydration of the system with 1 ml of $NaNO_3$ solution. From that, different solutions in the concentration range from 0.05 to 2 mg/ml were prepared. The R_h values of the polymer/Pro were measured using LS and QELS detectors and compared to the same concentration of polymer only.

Drug release study

Each HPG-C_n-MPEG/Pro solution (2 ml of 20 mg/ml) at a drug concentration of 250 µg/ml was filtered with a 0.2 µm syringe filter and then transferred into a dialysis cassette (molecular weight cut off 3500) and placed in a bottle containing 1 L of 10 mM PBS (pH 7.4) at 37 °C with slight agitation. The total

volume of the release medium was chosen such that when Pro was completely released, its concentration in the dialysate was below its solubility in water, which is 10.4 µg/ml at 37 ^{o}C .[41] At different time points, the concentration of Pro was measured by taking 75 µl of sample from the cassette, diluting into 2.25 ml ACN and assaying by UPLC, as described above. Both HPG-C_n-MPEG and Pro are very soluble in ACN; all the Pro appears in solution and is assayed as the free material by UPLC. Control mixtures combined Pro with HPG (HPG (M_n = 98,000) and the HPG-MPEG control described above for DSC measurements.

Release kinetics of drug from HPG-C_n-MPEGs were also studied in anticoagulated human platelet-poor plasma (PPP) to observe the effect of plasma proteins' interactions with Pro in the release profile. In this study, HPG-C_8-MPEG/Pro solutions (2 ml of 20 mg/ml) in PPP at the drug concentration of 250 µg/ml were transferred into dialysis cassettes (molecular weight cut off 3500) in a bottle containing 1 L of 10 mM PBS (pH 7.4) at 37 ^{o}C with slight agitation. At different time points, the concentration of Pro was measured by taking the sample from the dialysis bag as above, diluting 4 times with ACN, followed by centrifugation for removal of precipitated proteins to separate the top ACN layer and assayed by UPLC, as described above.

Results

Synthesis and characterization of HPG-C_n-MPEGs

We have reported previously the synthesis and biocompatibility of HPGs, modified with hydrophobic groups and MPEG chains prepared in a single-pot reaction strategy, based on anionic ring opening polymerization of epoxide based monomers.[10] These polymers have been shown to bind hydrophobic ligands, such as pyrene, fatty acids, docetaxel and paclitaxel.[10,34,38,39] For efficient drug loading, we modified some of the numerous hydroxyl end groups of growing HPGs with commercially available 1,2-epoxyalkane (C_n) in the range of 10-30% of the OH groups (n = 6, 8, 10, 12, 14) and 3% of the OH groups with C_{18}. The purpose was to incorporate as many alky chains into the polymeric system as possible in order to observe the effect of alkyl chain length on the drug encapsulation. To protect the hydrophobic constituents from causing aggregation and to increase the solubility of HPGs, polymers were then quantitatively modified with MPEG-epoxide 350 with conversion of 30-40% of hydroxyl groups but the alkylation process increased the polydispersity of the samples so fractionation was required to produce well defined materials

The polymers were characterized by proton NMR and GPC-MALLs. ^{1}H NMR showed the characteristic peaks of alkyl groups. Also, a peak corresponding to OCH_3 of MPEG-epoxide and the absence of any epoxide groups represented the absence of contamination of polymer by unreacted monomers. A quantitative estimation of glycidol groups and the composition was obtained in $CDCl_3$ (Figures S-2 and S-4). The molecular characteristics of these selected polymers with different compositions of hydrophobic groups and molecular weights are summarized in Table 1. The derivatized polymers have acceptable molecular weight distributions in the range 1.2-2 (Figure S-3 and Figure S-5). FTIR spectroscopy also confirmed the presence of C-O and O-H bonds (Figure S-6).

^{1}H NMR (300 MHz, $CDCl_3$) δ(ppm): 0.90 (3H, t, J = 6.0 Hz, CH_3 – from C_8 monomer); 1.25-1.50 (10H, m, CH_2 – from C_8 monomer); 3.50-3.95 (CH and CH_2 – from HPG core); 3.39 (3H, s, OCH_3 – from MPEG).

^{1}H NMR (300 MHz, $CDCl_3$) δ(ppm): 0.88 (3H, t, J = 6.0 Hz, CH_3 – from C_{12} monomer); 1.20-1.50 (18H, m, CH_2 – from C_{12} monomer); 3.50-3.95 (CH and CH_2 – from HPG core); 3.38 (3H, s, OCH_3 – from MPEG).

Inverse-gated ^{13}C NMR spectroscopy proves the branched structure of HPGs conjugated with alkyl chains and MPEG chains. The ^{13}C NMR spectrum of HPG-C_8-MPEG in methanol-d_4 is shown in Figure S-7.

Calculating degree of branching (DB) as reported previously, [43] confirms the branched structure of this polymer with the value of 0.61 through the following formulation:

$$DB = \frac{2D}{2D + L_{13} + L_{14}} \quad [4]$$

where: D is dendritic, T is terminal, L_{13} is linear (primary hydroxyl), and L_{14} is linear (secondary hydroxyl).

^{13}C NMR (400 MHz, methanol-d_4) δ(ppm): 14.72 (CH_3 – from alkyl on C_8 monomer); 23.87, 26.81, 30.74, 33.18 and 34.67 (CH_2 – from alkyl on C_8 monomer); 59.27 (OCH_3 – from MPEG); 62.99-81.53 (CH and CH_2 – from HPG core).

Drug encapsulation by HPG-C_n-MPEGs

The HPG-C_n-MPEG systems used here appear in solution as free nanoparticles < 10 nm in diameter (Table 1). Uncomplexed Pro is a hydrophobic drug with a low aqueous solubility of < 7.8 µg/ml at room temperature, 10.4 µg/ml at 37 °C at neutral pH; 1 mg/ml of HPG-C_n-MPEG (n = 8, 10, 12, 14) increased the aqueous solubility of Pro to ~ 20 µg/ml per milligram of polymer. The maximum loaded amount was 325 µg/ml of Pro which was bound by most of the polymer systems, including HPG-C_n-MPEGs containing C_8, C_{10}, C_{12} and C_{14} alkyl monomers with different molar ratios determining the hydrophobicity of the polymer (Figure 2). However, lower amounts of alkylation were found for HPG-C_n-MPEG (n = 6 and 18). This maximum binding corresponded to a ratio of 8.1 moles of drug per mole of polymer for the HPG-C_{12}-MPEG/Pro system for instance; the full set of values is given in Table 2 and contextualized under Discussion. The combinations that fell along the unit slope line of Fig. 2 and did not produce any Pro precipitation over 12 hr at room temperature were considered stable; only the HPG-C_6-MPEG materials showed instability by this criterion.

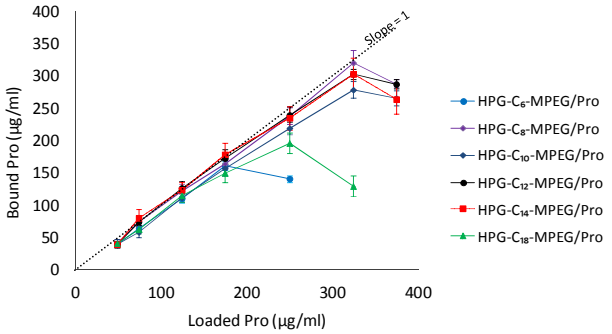

Figure 2. Pro binding profile into HPG-C_n-MPEGs in PBS

Table 2. Binding characteristics of HPG-C_n-MPEGs

Sample	No. of hydrophobic carbons per molecule (n-2)	Maximum molar ratio (drug/polymer)
HPG-C_6-MPEG/Pro	460	1.7
HPG-C_8-MPEG/Pro	822	5.1
HPG-C_{10}-MPEG/Pro	712	4.8
HPG-C_{12}-MPEG/Pro	1110	8.1
HPG-C_{14}-MPEG/Pro	720	6.0
HPG-C_{18}-MPEG/Pro	272	3.5

***In vitro* release study**

To evaluate HPG-C_n-MPEGs' potential as drug carriers, the release of Pro from the polymeric systems was measured at 37 °C in PBS through a dialysis method. HPG-C_6-MPEG was omitted from this study due to the lack of long term stability of the carrier loaded with Pro. The HPG-C_n-MPEG/Pro solutions in PBS at the drug concentration of 250 μg/ml were transferred into dialysis cassettes (molecular weight cut off 3500) in a bottle containing 1 L of 10 mM PBS (PH 7.4) at 37 °C with slight agitation. At different time points, the concentration of Pro was measured by taking the sample from the bag, diluted in ACN and assayed by UPLC, as described above. Comparing the release profiles of all HPG-C_n-MPEG/Pro systems, the slowest release profile belongs to HPG-C_8-MPEG/Pro, in which about 60% of the drug is released in the first 8 hrs and about 98% is released within 5 days; this compares with HPG-C_{18}-MPEG/Pro which released ~ 80% in the first 8 hrs. Unbound drug clearance, as well as drug release in the presence of HPG and HPG-PEG, from the dialysis cassette were also measured as controls in order to observe the effect of alkylation on release behaviour. This was done by adding 2 ml PBS containing 5 μg of free drug to the cassette followed by dialyzing against PBS and analyzing the contents (Figure 3).

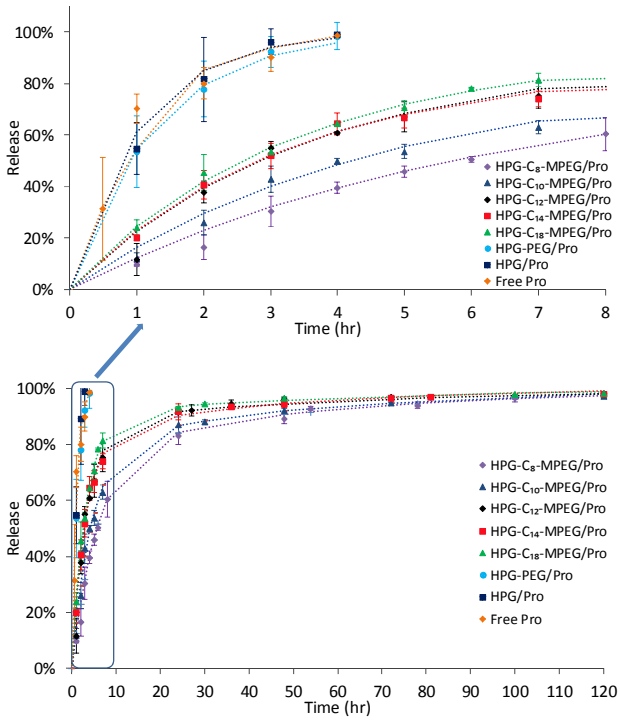

Figure 3. Pro release from HPG-C_n-MPEGs in PBS

The release profiles of Pro from HPG-C_n-MPEGs occurred in two phases, a rapid phase over the first 8-10 hrs followed by slower release which continued for several days. To compare the release rate for each polymer-drug system, we measured the rate at which the drug left the dialysis cassette by diffusion into the media. For each HPG-C_n-MPEG species we found that the natural log (ln) of drug concentration versus time plot was not a straight line as predicted for simple first order drug release and elimination.

Release from HPG-C_8-MPEG/Pro in PBS: this profile demonstrated that two linear regions were observed, an early rapid release of ~ 60-75% of the bound drug occurred over the first ~ 8 hrs followed by a much slower phase which was again linear on the semi-log plot. These general features were observed for all of the HPG-C_n-MPEG/Pro systems studied. Pro diffusion out of the cassette in the absence of HPG-C_n-MPEG proceeded most rapidly and with only one first order rate, as would be expected since the initial concentration of the drug ensured it was initially fully in solution. We characterize the two phases of release with two rate constants, calculated from the slopes of the two linear portions of the semi-log plots of each HPG-C_n-MPEG/Pro system; the total time course for HPG-C_8-MPEG/Pro is illustrated in Figure 4 and the individual phases analyzed in Figures S-8 and S-9 in Supporting Information; the rate constants derived from these two figures are recorded in Table 3.

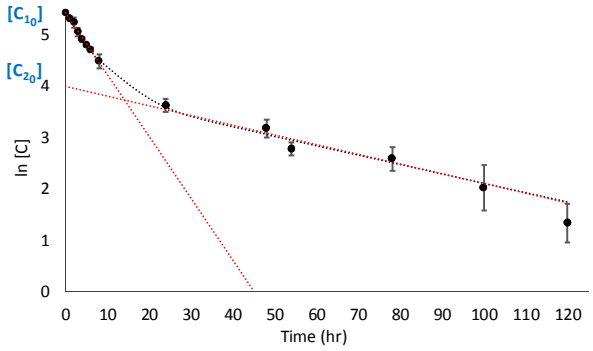

Figure 4. Semi-log plot illustrating the kinetics of Pro release from HPG-C_8-MPEG/Pro. [C] refers to Pro concentration. [C_{1_0}] is the initial Pro concentration, calculated from the intercept of the ln[Pro] versus time in the rapid release phase. [C_{2_0}] is the initial Pro concentration for the slow release phase, calculated from the intercept of the ln[Pro] versus time at later times.

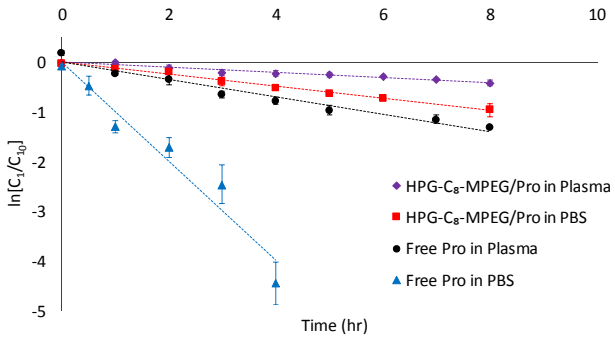

Figure 5. Semi-log plots of the initial phase of release of Pro from the dialysis cassettes for HPG-C_8-MPEG/Pro in plasma (R^2 = 0.96) and for dissolved Pro alone in PBS (R^2 = 0.95) and plasma (R^2 = 0.95). [C_1] is the ln of Pro concentration vs. time in the rapid release phase. [C_{1_0}] is the initial Pro concentration, calculated from the intercept of ln [C_1] vs. time.

Table 3. Pro release rate constants from HPG-C_n-MPEGs

Sample	k_1 (10^{-6} s^{-1}) Rapid-release phase rate constant in PBS	k_2 (10^{-6} s^{-1}) Slow-release phase rate constant in PBS
HPG-C_8-MPEG/Pro	33.4 ± 1.1	0.6 ± 0.5
HPG-C_{10}-MPEG/Pro	41.1 ± 3.1	0.5 ± 0.3
HPG-C_{12}-MPEG/Pro	58.7 ± 4.6	0.3 ± 0.7
HPG-C_{14}-MPEG/Pro	55.4 ± 5.0	0.4 ± 0.2
HPG-C_{18}-MPEG/Pro	66.5 ± 2.1	0.4 ± 0.5
HPG/Pro	326 ± 26.8	N/A
HPG-MPEG/Pro	274 ± 24.8	N/A
Free Pro	275.5 ± 32.8	N/A

For any *in vivo* experiments or clinical applications in humans, HPG-C_n-MPEG/Pro would encounter blood plasma before reaching target organs so the release rate of Pro exposed to PPP was also studied for the HPG-C_8-MPEG/Pro system and release rates compared to PBS (Table 4).

Table 4. Pro release rate constants from HPG-C_8-MPEG in plasma vs. PBS

Sample	k_1 (10^{-6} s^{-1}) in plasma	k_2 (10^{-6} s^{-1}) in plasma	k_1 (10^{-6} s^{-1}) in PBS	k_2 (10^{-6} s^{-1}) in PBS
dHPG(C_8)/Pro	14.3 ± 1.1	0.6 ± 0.4	33.4 ± 1.1	0.6 ± 0.5
Free Pro	48.5 ± 4.4	0.4 ± 0.8	275.5 ± 32.8	N/A

The semi-log plot showing release kinetics in plasma is illustrated in Figure S-10 where again it is seen that release occurs in two linear phases but with different slopes from those measured in PBS (Figure 5). A direct comparison of the initial behaviour in both solutions is given in Figure 5; release behaviour of Pro dissolved in each solution in the absence of HPG-C_n-MPEG is also included.

Correlations between chemical properties and loading or release

While it seems clear from our previous experience that the inherent hydrophobicity of the modified polymers will affect the binding of hydrophobic drugs, access to the present set of HPG-C_n-MPEGs allows a more detailed examination of the molecular determinants of binding and release of Pro by this family of materials. The reduced synthetic control compared to pure HPGs combined with the necessary product fractionation provided a larger range in properties than might have seemed desirable but allowed us to look at contributions to the binding and release metrics from several sources. The independent variables that were considered were the number of alkyl carbons per HPG-C_n-MPEG molecule, the number of purely hydrophobic alkyl carbons per molecule (explained below), the volume expected to be occupied by the alkyl chains if they accumulated into a drop-like region in the interior of the polymer to minimize aqueous contact, and the volume of the HPG contribution to the HPG-C_n-MPEG to see if the molecular size of the hydrophilic polymer played any role.

We proceeded by looking for correlations between the above variables and either the capacity of each HPG-C_n-MPEG species to bind Pro or the values of the two kinetic constants describing Pro release rates into buffer (Tables 2 and 3). The results of linear regression analysis among these parameters are given in Table 5.

The strongest correlation ($p < 0.03$) for the Pro loading capacity of HPG-C_n-MPEGs was found with the number of alkyl carbons per molecule beyond the oxygen molecule originating from the epoxide oxygen of the monomer, which is given by (n-2) where n is the total number of carbon atoms in the alkyl epoxide monomer. This value represents more accurately the pure hydrophobic carbon chain size for each monomer and could be relevant to the strength of hydrophobic interaction per alkyl unit contributing to Pro binding. The linear regression between Pro loading and n was not significant, lending some support to this idea.

Maximum Pro loading was not significantly correlated with the volume contributed by alkyl carbons, $V_{a(n-2)}$. Pro loading takes

place in the absence of water however so an oil-like core with a significant interfacial tension that could act as a solvent reservoir for the hormone would not be anticipated.

Table 5 shows that the release rate constants for Pro, k_1 and k_2, correlated significantly only with the volume of the polymer V_p and the volume of the polymer with the alkyl contribution subtracted ($V_p - V_{a(n-2)}$; Figure S-11). Surprisingly, there was no direct correlation of the release rate constants with any of the parameters describing the alkyl content.

Since we have no evidence that Pro binds to HPG itself, the dependence on the hydrodynamic volume of the polymer was unexpected. However, it has been shown that HPG interacts with water in a substantial way and that in the presence of HPG a fraction of the water in a solution does not participate in freeze/thaw heat exchange around T = 0 °C.[37,38] The solutions behave as if a significant amount of water was bound or otherwise structured in a way distinct from pure water when HPG is present. If this bound or structured non-freezing water had different solution properties for Pro an effect on the release kinetics of Pro from HPG-C_n-MPEGs might occur.

Table 5. Summary of linear regression analysis (regression coefficient R^2 and significance probability p) examining the dependence of maximum Pro capacity and two kinetic constants for Pro release

N=5	No. $C_{(n)}$ [a]		No. $C_{(n-2)}$ [b]		$V_{a(n-2)}$ [c]		V_p [d]		V_p-$V_{a(n-2)}$ [e]	
	R^2	p	R^2	p	R^2	p	R^2	p	R^2	p
Max Pro per HPG-C_n-MPEG [f]	0.559	0.087	0.743	**0.027**	0.710	0.073	0.119	0.57	0.111	0.58
k_1	0.211	0.436	0.119	0.570	0.220	0.43	0.880	**0.018**	0.889	**0.016**
k_2	0.033	0.770	0.003	0.934	0.038	0.75	0.863	**0.022**	0.863	**0.022**

[a]: Number of alkyl carbon atoms per HPG-Cn-MPEG molecule. [b]: Number of n-alkyl carbons external to oxygen per HPG-C_n-MPEG molecule. [c]: Volume of n-alkyl carbons external to oxygen per HPG-C_n-MPEG molecule. [d]: Volume of HPG-C_n-MPEG molecule calculated from hydrodynamic radius. [e]: Volume of HPG-C_n-MPEG molecule associated with HPG. [f]: Maximum ratio of Pro bound to HPG-C_n-MPEG by loading protocol, moles per mole; $p < 0.05$ values in bold font. See text for fuller definitions

To test this idea we performed DSC measurements on the series of HPG-C_n-MPEG species under investigation, as described. The results are shown in Table 6 where the reduction in heat of fusion measured as a function of HPG-C_n-MPEG structure and concentration is interpreted in terms of number of moles of water affected per mole of polymer.

Table 6. Summary of DSC results: number of moles of water affected per mole of HPG-C_n-MPEG at the two polymer concentrations shown

HPG-C_n-MPEG	Mole water per mole 10% HPG-C_n-MPEG (10^3)	Mole water per mole 5% HPG-C_n-MPEG (10^3)
HPG-C_8-MPEG	6.3	5.2
HPG-C_{10}-MPEG	6.9	8.4
HPG-C_{12}-MPEG	8.2	11.4
HPG-C_{14}-MPEG	9.4	10.6
HPG-C_{18}-MPEG	12.6	15.4
HPG-MPEG	13.9	17.9

We also studied Pro release from HPG-C_8-MPEG system in plasma using the above method. Comparison of the kinetics of release in PBS and plasma showed that the release rate of Pro from HPG-C_8-MPEG/Pro was reduced to almost half in plasma and the release of free drug with no HPG-C_n-MPEG present now showed two phases unlike the situation in PBS, presumably due to Pro reversibly binding to plasma constituents before diffusing out of the cassette. There was an approximately 20 fold difference in k_1 between free Pro in PBS compared to Pro bound to HPG-C_8-MPEG in plasma (Figure 5 and Table 4). We did not attempt a more detailed examination of plasma effects in this work as its composition varies widely depending on donor issues related to genetic background, gender, health status, diet and degree of fasting so attempting a deeper understanding would take us beyond the scope of this work.

When the results of the DSC measurements were examined for correlation with the kinetic constants for Pro release from the HPG-C_n-MPEG species the regression analyses summarized in Table 7 were obtained.

Table 7. Summary of linear regressions of k_1 and k_2 against the number of moles of water affected per mole of HPG-C_n-MPEG as determined by DSC

N=5	Water/ HPG-C_n-MPEG [a] (10 %)		Water/ HPG-C_8-MPEG [b] (5 %)		(n-2) [c]	
	R^2	p	R^2	p	R^2	p
k_1	0.793	**0.043**	0.940	**0.006**	0.857	**0.024**
k_2	0.392	0.258	0.720	0.069	0.501	0.181

[a]: HPG-C_n-MPEG concentration of 10%. [b]: HPG-C_n-MPEG concentration of 5 %. [c]: the number of alkyl carbons external to the oxygen for each monomer species; statistically significant results in bold

It is seen the most significant correlation is between k_1 and the number of moles of water affected per mole of HPG-C_n-MPEG at the lower polymer concentration; detailed plots are shown in Figure 6. A higher but still significant p value ($p < 0.025$) is found for the correlation with simply the length of the hydrophobic portion of the alkyl monomers, (n-2), which could also reflect an effect of structured water around the alkyl chains. The k_2 values do not correlate significantly with the water-related parameters, although there is some suggestion

that k_2 tracks with the water affected at the lower concentration. Since the release kinetics took place from 2% polymer solutions the 5% water binding data is likely the most relevant. Note that the two dependences are of opposite sign however, k_1 increasing as the amount of water affected increases with alkyl chain length while k_2 decreases over the same range.

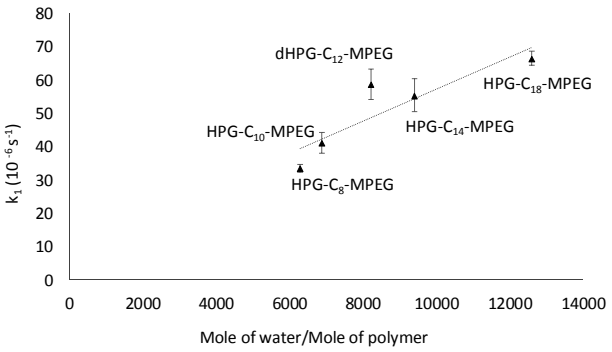

Figure 6. Correlation between k_1 values and mole of structured water per mole of HPG-C_n-MPEG at 5% polymer concentration; $R^2 = 0.94$ and $p < 0.01$

Discussion

In this study, we describe the development of a nanoparticulate formulation for Pro delivery based on HPGs containing hydrophobic groups within the structure and MPEG chains incorporated in the polymer (presumably on the surface). Our approach was based on HPGs because of their ease of synthesis and excellent biocompatibility.[24,27] The HPG-C_{18}-MPEG material has been shown to be non-toxic in mice and capable of being retained for extended periods of time in the circulation depending on the molecular weight so holds considerable promise as a drug delivery agent.[10,26] In synthesizing this family of polymers the 1,2-epoxyalkane (C_n) was added to the activated initiator with the glycidol to try to provide a protected hydrophobic region that would not produce aggregation in aqueous solution but would provide a suitable environment for Pro binding. While such materials are usually thought of as having a hydrophobic core it is not clear how much the alkyl chains can interact with each other given the constraints of the dendritic structure of the polymer and if in fact they do form an oily central region with an identifiable interface with water.

The materials synthesized as described successfully bound Pro and released it into aqueous media. The capacity of these polymers to bind Pro depended on the extent and chain length of the alkyl epoxides used in the synthesis. Table 2 and Figure S-12 show that the best correlation between loading capacity and a structural property was the dependence on the sum per HPG-C_n-MPEG molecule of the number of carbon atoms in the alkyl units external to the oxygen contributed from the epoxide group, two less than the number of carbons in the alkyl monomers (n). The HPG-C_{12}-MPEG had the highest value for this parameter and the highest loading capacity. The correlation implies the hydrophobic group length was a strong determinant of loading capacity. Since the loading occurs in the absence of water this is perhaps not surprising as there would be little change in free energy to be gained if the alkyl chains accumulated in the absence of an aqueous interface with a relatively high interfacial tension. In such a case a dependence on the summed volume of the hydrophobic chains, roughly equal to a core drop volume into which the Pro could dissolve, might have been expected yet the dependence of loading on $V_{a(n-2)}$, which is the relevant measure, is not significant.

Results from our earlier work and the R_h values demonstrated that loading Pro on HPG-C_n-MPEG does not cause aggregation in the system and no change in the size of the dominant population was observed at different concentrations compared to the polymer alone at the same concentrations as a control. This confirms the non-micelle structure of HPG-C_n-MPEG (Table S-1 and Figure S-13). In earlier work we showed this class of materials could actually collapse around a hydrophobic guest molecule, protecting against aggregation in aqueous solution and that their capacity to solubilize a hydrophobic guest[11] was a linear function of polymer concentration over a much greater concentration range than used in this research so no micelle-enhancement of binding was expected[10]. The very scant population of weak aggregates seen in the present material also reduced its mean size on binding Pro, consistent with our earlier findings[11].

It has been previously demonstrated that more hydrophilic drugs are released more rapidly from the polymer matrix as water penetrates into it.[39] Pro release occurred in two phases, each of which could be characterized by a first order kinetic constant. The initial phase was the most rapid and its kinetic constant, k_1, was roughly 5 to 20 times greater than k_2 characterizing the second phase. When correlations were sought with system properties, very different results were found compared to the loading capacity determinants, the character of hydration of the dendritic material being the dominant feature. Table 7 and Figure S-11 show some results: both k_1 and k_2 are significantly correlated ($p < 0.025$) with the hydrated polymer volume (calculated from the hydrodynamic radius), corrected or not for the alkyl chain volume. Since we have no evidence for Pro binding to HPG-MPEG, and there was no correlation of loading capacity determined in the absence of water with polymer volume, it seemed likely the hydration of the polymer could be involved.

The DSC measurements subsequently made brought some clarity to the situation as significant reductions in the heat absorbed during thawing were found when the HPG-C_n-MPEGs were present, implying a fraction of the water present did not freeze and was either bound to polymer or structured in some way that did not contribute to melting as the temperature was raised through 0 °C. From this observation the amount of water affected can be calculated; Table 6 gives the results expressed as moles of water affected per mole of HPG-C_n-MPEG. It is of interest that the amounts of water affected by the HPG-C_n-MPEGs were much more per monomer than has been observed in other related linear polymer systems, including PEG,[44,45] perhaps due to the dendritic nature and high internal

chain density of HPG. Seeking a correlation between these properties and the kinetic constants rendered the results given in Table 7 and Figure 6. A very strong correlation ($p = 0.006$) is found between k_1 and the moles of water bound or structured per mole of HPG-C_n-MPEG at 5% polymer concentration, and a still significant ($p < 0.05$) correlation at 10%. As noted earlier the lower concentration is closer to the experimental conditions used in the kinetic measurements so is the more relevant. Figure 6 and the regression (Table 7) show that k_1 increases significantly as the amount of affected water increases, perhaps suggesting that the affected water forms a better solvent for Pro than bulk water, enhancing its release from whatever binding interaction retains it.

The second phase kinetic constant, k_2, has the opposite slope in its correlation with the affected water parameter but does not reach significance. This much slower release process occurs at quite low remaining loads so could reflect a small population of material slightly more tightly associated with the HPG-C_n-MPEG, perhaps due to proximity of alkyl chains within the polymer. It might also be associated with the weakly aggregated population present at low levels under low shear conditions[11] (Fig S-13). Since k_1 also correlates quite well ($p < 0.025$) with simply the number of alkane carbons external to the oxygen in the alkyl monomer (Table 7) it suggests that a contribution to the affected water could be associated with the alkane chain length, consistent with the hydrophobic effect [46] playing a role in the thermodynamic behaviour of the entrained water.

Conclusions

Delivery of hydrophobic drugs to therapeutic sites is one of the major research challenges in pharmaceutical science due to their poor aqueous solubility. Several formulations, including micelles, have been studied in detail, and unimolecular micelles are being considered as very promising carriers due to their structural stability. In this study, we report the preparation and characterization of Pro carriers in a nanoparticulate formulation based on hydrophobically derivatized hyperbranched polyglycerols. The maximum binding capacity for Pro, loaded in the absence of water, was found to depend on the total mass of alkyl carbon per molecule, not on the volume of hydrophobic constituents. The release rates from HPG-C_n-MPEGs for Pro could be characterized by two kinetic constants, the major one correlating with the volume of the hydrated polymer and more directly, as shown by DSC measurements, with the amount of water structurally affected per mole of polymer. Pro release in human plasma was slower than in buffer but had the same general characteristics. These studies provide insight into the nature of binding of a hydrophobic drug into alkylated HPGs and permit a connection to be drawn between the release rates and the amount of bound or structured water associated with the polymers. They hence offer some guidelines for the design of Pro carriers with some control over loading and release properties.

Acknowledgements

We would like to thank Dr. Johan Janzen and Irina Chafeeva for their excellent technical assistance, Dr. Jay Kizhakkedathu for ongoing discussion and Dr. Rajesh Shenoi for helpful advice. We also would like to thank Dr. Lawrence Amankwa and Dr. Clement Mugabe at Centre for Drug Research and Development at UBC for the outstanding UPLC method they have developed, which we employed for the binding and releasing study. This research was supported by a Discovery Grant to D.E.B. from the Natural Sciences and Engineering Research Council Canada and benefited from infrastructure in the UBC Centre for Blood Research funded by the Canada Foundation for Innovation and the BC Knowledge Development Fund.

Notes and references

1 E. H. Andersson, R. Bjorklund, I. Emanuelson and D. Stalhammar, *Acta Neurol. Scand.,* 2003, **107**, 256-259.
2 J. A. Mortimer, C. M. Duijn, V. Chandra, L. Fratiglioni, A. B. Graves, A. Heyman, A. F. Jorm, E. Kokemen, K. Kondo, W. A. Rocca. S. H. Shalat, H. Soininen and A. Hofman, *Int. J. Epidemiol.,* 1991, **20 Suppl 2**, S28-S35.
3 S. Corkin, T. J. Rosen, E. V. Sullivan and R. A. Clegg, *J. Neurosci.* 1989, **9**, 3876-3883.
4 S. Thornhill, G. M. Teasdal, G. D. Murray, J. McEwen. C. W. Roy and K. Penny, *BMJ,* 2000, **320**, 1631-1635.
5 J. W.Finnie and P. C. Blumbergs, *Vet. Pathol*., 2002, **39**, 679-689.
6 D. I. Graham, T. K. McIntosh, W. L. Maxwell and J. A. R. Nicoll, *J. Neuropathol., Exp. Neurol*., 2000, **59**, 641-651.
7 I. Roberts, G. Schierhout and P. Alderson, *J. Neurol. Neurosurg. Psychiat.,* 1998, **65**, 729-733.
8 D. B. Guthrie, D. G. Stein, D. C. Liotta, M. A. Lockwood, I. Sayeed, F. Atif, R. F, Arrendale, G. Prabhakar Reddy, T. J. Evers, J. R. Marengo, R. B., Howard, D. G. Culver and M. G. Natchus, *Med. Chem. Lett.,* 2012, **3**, 362-366.
9 D. W. Wright, A. L. Kellermann, V. S. Hertzberg, P. L. Clark, M. Frankel, F. C. Goldstein, J. P. Salomone, L. L. Dent. O. A. Harris, D. S. Ander, D. W. Lowery, M. M. Patel, D. D. Denson, A. B. Gordon, M. M. Wald, S. Gupta, S. W. Hoffman and D. G. Stein, *Annals of Emergency Medicine,* 2007, **49**, 391-402.
10 R. K. Kainthan, J. Janzen, J. N. Kizhakkedathu, D. V. Devine and D. E. Brooks, *Biomaterials,* 2008, **29**, 1693-1704.
11 R. K. Kainthan, C. Mugabe, H. M. Burt and D. E. Brooks, *Biomacromolecules,* 2008, **9**, 886-895.
12 G. S. Kwon and K. Kataoka, *Adv. Drug Delivery Rev*., 1995, **16**, 295-309.
13 M. Jones and J. Leroux, *Euro. J. Pharm. Biopharm*., 1999, **48**, 101-111.
14 V. P. Torchilin, *J. Controlled Release,* 2001, **73**, 137-172.
15 G. Riess, *Prog. Polym. Sci.,* 2003, **28**, 1107-1170.
16 G. R. Newkome, C. N. Moorefield, G. R. Baker, M. J. Saunders and S. H. Grossman, *Ang. Chem. Int. Ed. Engl*., 1991, **30**, 1178-1180.
17 H. Liu, S. Farrell and K. Uhrich, *J. Controlled Release,* 2000, **68**, 167-174.
18 M. Liu, K. Kono and J. M. J. Frechet, *J. Controlled Release*, 2000, **65**, 121-13118
19 C. J. Hawker, K. L. Wooley and J. M. J. Frechet, *J. Chem. Soc., Perkin. Trans.,* 1993, **1**, 1287-1297.
20 A. Heise, J. L. Hedrick, C. W. Frank and R. D. Miller, *J. Am. Chem. Soc.,* 1999, **121**, 8647-8648

21 N. K. Jain and U. Gupta, *Expert Opin. Drug Metab. & Toxicol.*, 2008, **4**, 1035-1052.
22 T. Satoh, *Soft Matter*, 2009, **5**, 1972-1982.
23 R. K. Kainthan, M. Gnanamani, M. Ganguli, T. Ghosh, D. E. Brooks, S. Maiti and J. N. Kizhakkedathu, *Biomaterials*, 2006, **27**, 5377-5390.
24 R. K. Kainthan, J. Janzen, E. Levin, D. V. Devine and D. E. Brooks, *Biomacromolecules,* 2006, **7**, 703-709.
25 R. K. Kainthan, E. B. Muliawan, S. G. Hatzikiriakos and D. E. Brooks, *Macromolecules,* 2006, **39**, 7708-7717.
26 R. K. Kainthan and D. E. Brooks, *Biomaterials*, 2007, **28**, 4779-4787.
27 R. K. Kainthan, S. R. Hester, E. Levin, S. R. Hester, E. Levin, D. V. Devine and D. E. Brooks, *Biomaterials*, 2007, **28**, 4581-4590.
28 R. K. Kainthan and D. E. Brooks, *Bioconjugate Chem.*, 2008, **19**, 2231-2238.
29 N. A. A. Rossi, I. Mustafa, J. K. Jackson, H. M. Burt, S. A. Horte, M. D. Scott and J. N. Kizhakkedathu, *Biomaterials,* 2009, **30**, 638-48.
30 N. A. A. Rossi, I. Constantinescu, R. K. Kainthan, D. E. Brooks, M. D. Scott and J. N. Kizhakkedathu, *Biomaterials,* 2010, **31**, 4167-4178.
31 N. A. A. Rossi, I. Constantinescu, D. E. Brooks, M. D. Scott and J. N. Kizhakkedathu, *J. Am. Chem. Soc.,* 2010, **132**, 3423-3430.
32 Z. Liu, J. Janzen and D. E. Brooks, *Biomaterials*, 2010, **31**, 3364-3373.
33 J. G. Zhang, O. B. Krajden, R. K. Kainthan, J. N. Kizhakkedathu, I, Constantinescu, D. E. Brooks and M. I. Gyongyossy-Issa, *Bioconjugate Chem.,* 2008, **19**, 1241-1247.
34 C. Mugabe, B. A. Hadaschik, R. K. Kainthan, D. E. Brooks, A. I. So, M. E. Gleave and H. M. Burt, *BJU Int.,* 2008, **103**, 978-986.
35 R. A. Shenoi, B. F. L. Lai, M. I. Ul-haq, D. E. Brooks and J. N. Kizhakkedathu, *Biomaterials*, 2013, **34**, 6068-6081.
36 C. Du, A. A. Mendelson, Q. Guan, R. Chapanian, I. Chafeeva, G. da Roza and J. N. Kizhakkedathu, *Biomaterials,* 2014, **35**, 1378-1389.
37 R. Chapanian, I. Constantinescu, N. A.A. Rossi, N. Medvedev, D. E. Brooks. M. D. Scott and J. N. Kizhakkedathu, *Biomaterials,* 2012, **33**, 7871-7883.
38 C. Mugabe, P. A. Raven, L. Fazli, J. H. E. Baker, J. K. Jackson, R. T. Liggins, A. I. So, M. E. Gleave, A. I. Minchinton, D. E. Brooks and H. M. Burt, *Biomaterials*, 2012, **33**, 692-703.
39 C. Mugabe, R. T. Liggins, D. Guan, I. Manisali, I. Chafeeva, D. E. Brooks, M. Heller, J. K. Jackson and H. M. Burt, *Int. J. Pharm.,* 2011, **404**, 238-249.
40 M.R. Radowski, A. Shukla, H. von Berlepsch, C. Bttcher, G. Piickaert, H. Rehage and R. Haag, *Angewandte Chemie*, 2007, **46**, 1265-1269.
41 H. Hong, Y. Mai, Y. Zhou, D. Yuan and J. Cui, *Macromol. Rapid Commun.,* 2007, **28**, 591-596.
42 L. Song, Studies of solubilization of poorly water-soluble drugs during in vitro lipolysis of a model lipid-based drug delivery system and in mixed micelles (Unpublished doctoral dissertation). University of KentuckySong, Lexington, KY, 2011.
43 A. Sunder, R. Hanselmann, H. Frey and R. Mülhaupt, *Macromolecules,* 1999, **32**, 4240-4246.
44 M. Tanaka, T. Hayashi and S. Morita, *Polym. J.*, 2013, **45**, 701-710.
45 O. Tirosh, Y. Berenholz, J. Katzhendler and A. Priev, *Biophys. J.*, 1998, **74**, 1371-1379.
46 C. Tanford, The hydrophobic effect: formation of micelles and biological membranes, 2nd ed; A Wiley-Interscience publication, New York, NY, 1979.